

RESEARCH MEMORANDUM

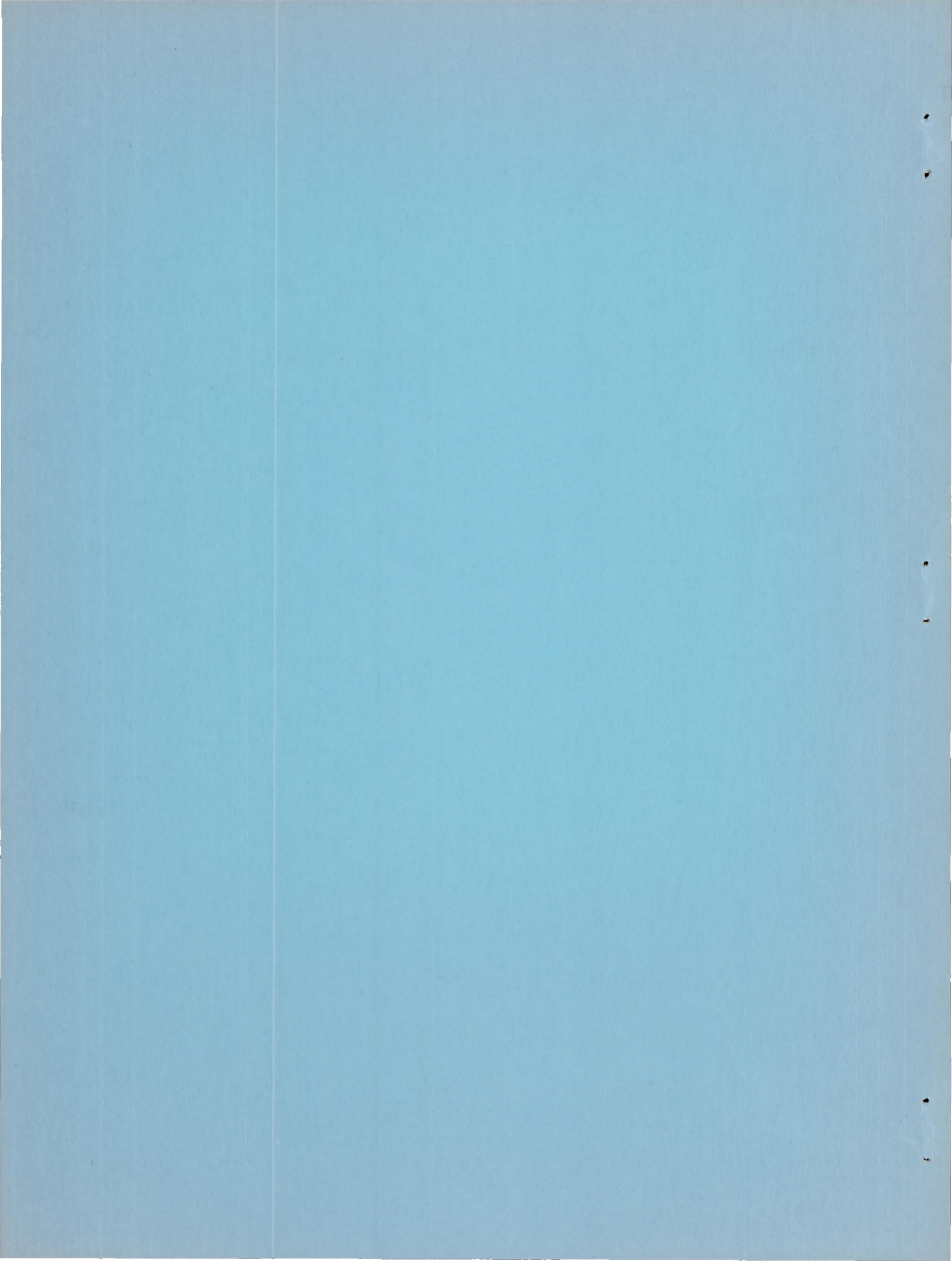
ENGINE PERFORMANCE OF PRECISION-FORGED, ELECTROPOLISHED
AND MACHINED BLADES OF NIMONIC 80 AND 80A ALLOYS

By Paul F. Sikora and James R. Johnston

Lewis Flight Propulsion Laboratory
Cleveland, Ohio

NATIONAL ADVISORY COMMITTEE
FOR AERONAUTICS
WASHINGTON

April 5, 1955
Declassified February 8, 1957



NATIONAL ADVISORY COMMITTEE FOR AERONAUTICS

RESEARCH MEMORANDUM

ENGINE PERFORMANCE OF PRECISION-FORGED, ELECTROPOLISHED,
AND MACHINED BLADES OF NIMONIC 80 AND 80A ALLOYS

By Paul F. Sikora and James R. Johnston

SUMMARY

An investigation was conducted to determine the effect of electropolishing precision-forged blades and of machining blades from oversize forgings on the engine performance of Nimonic 80 and Nimonic 80A turbine blades. These blades, along with precision-forged blades, were run in a J33-9 turbojet engine. The tests resulted in the following conclusions:

(1) Electropolishing of precision-forged blades did not improve engine life relative to the life of nonelectropolished blades.

(2) Machining blades from oversize forgings did not improve the engine life of precision-forged blades.

(3) The precision-forging and heat-treating practice used in fabricating the blades investigated was such that the surface roughness and oxide penetration was so slight, approximately 0.0005 inch in depth, as to preclude any benefits derived from surface removal by electropolishing or machining.

INTRODUCTION

Nickel-base alloys, such as Nimonic 80 and 80A, have been shown to be susceptible to surface oxidation (refs. 1 to 3). In addition, the cold-worked edges, recrystallized areas, and depletion zones that form at the surfaces of these alloys prior to or during high-temperature use are considered harmful. The removal of these deleterious surface effects may be accomplished by electropolishing after precision forging. In a previous investigation at the NACA Lewis laboratory (ref. 4), the blade performance of several forged nickel-base alloys was not improved by electropolishing.

Machining oversize forged blades is another method of surface removal that has been beneficial, especially under fatigue conditions. A substantial increase in the fatigue strength of Nimonic 80 turbine blades machined from forged slugs over that of precision-forged blades was reported in reference 5. Consequently, this investigation was conducted to determine:

- (1) The effect of electropolishing on the engine performance of Nimonic 80 and 80A turbine blades
- (2) The effect of machining on the engine performance of oversize forged Nimonic 80 turbine blades

Two lots of Nimonic 80 and one lot of Nimonic 80A blades were precision forged. One-half of each lot of blades was electropolished. One additional lot of Nimonic 80 (lot 2) blades was forged oversize and then machined to size. These blades were then operated in a J33-9 turbojet engine at the NACA Lewis laboratory. The test consisted of a repetition of a 20-minute cycle (15 min at rated speed and 5 min at idle speed). At rated speed, the blade temperature was maintained at 1500° F. Cyclic operation was employed to simulate service conditions.

MATERIALS, APPARATUS, AND PROCEDURE

Turbine Blades

The chemical compositions of the alloys investigated are listed in table I. Blades of the different alloys were evaluated at the conditions shown in the following table:

Group	Alloy	Number of blades	Condition of blades
1	Nimonic 80 (lot 1)	6	Precision forged
2	Nimonic 80 (lot 1)	6	Forged and electropolished
3	Nimonic 80A	6	Precision forged
4	Nimonic 80A	6	Forged and electropolished
5	Nimonic 80 (lot 2)	6	Precision forged
6	Nimonic 80 (lot 2)	6	Forged and electropolished
7	Nimonic 80 (lot 2)	6	Forged 0.030 in. oversize and machined to size
8	Haynes Stellite 21	10	Standard stock
		Total, 52	

The bar stock used in forging these blades was produced in England in accordance with Ministry of Supply Specifications D.T.D. 725 (Nimonic 80) and D.T.D. 736 (Nimonic 80A). The blades were forged as shown in

table II in the United States. Upon receipt of the blades at the Lewis laboratory, it was found that the leading and trailing edges of all blades had been left in the trimmed conditions. Therefore, it was necessary that the edges of all the blades be ground to shape and the blades of groups 2, 4, and 6 be re-electropolished. The blades of group 7 were machined to size on a pantographic multispindle grinder.

The electropolishing procedure employed on the blades of groups 2, 4, and 6 to remove approximately 0.001 inch was as follows:

Bath, percent phosphoric acid (H_3PO_4) by volume	75
Bath temperature, $^{\circ}F$	160-170
Current, amps/blade airfoil (16 sq in.)	60
Time, min	15-20

Prior to engine operation, the blades were inspected radiographically and visually using a fluorescent-oil penetrant method and were sound.

Stress and Temperature Distribution in Turbine Blades

During Engine Operation

The cross-sectional areas of several blades of each group were measured on an optical comparator prior to engine operation, and the stress distribution along the airfoil was calculated by the method described in reference 5.

Temperature measurements were made on two thermocoupled blades as described in reference 6.

On the basis of the stress and temperature distribution, a plot of stress-rupture life was determined for the conditions at each increment of blade length as shown in figure 1. From this stress-rupture plot, it may be seen that a zone of the blade, if subjected to stress-rupture conditions alone, exists where the blade life should be a minimum. This zone lies between 2 and $2\frac{1}{2}$ inches above the base.

Engine Operation

The test blades were installed in a J33-9 turbojet engine having a nominal thrust of 4000 pounds and employing a dual-entry centrifugal compressor. The engine and test instrumentation is described in reference 7. The engine test consisted of a repetition of the cycle shown in figure 2. During the rated-speed portion of the cycle, the

gas temperature was varied to yield a midpoint blade temperature of 1500° F. Blade stresses during the rated-speed portion of the cycle are shown in figure 1.

All blades were operated to failure (defined as either complete fracture or evidence of the beginning of fracture). In order to minimize the damage resulting from blade failure, the thickness of the shroud band in the engine tail cone that surrounds the turbine wheel was reduced to allow blade fragments to pierce the shroud band easily and to be thrown clear of the turbine. After each failure the blades were examined for damage, and the location and nature of the damage were recorded.

Blade-Elongation Measurements

Two blades of each group were scribed in the manner shown in figure 3. At engine shutdown periods, measurements were made of blade elongation between the scribe marks using an optical extensometer.

Metallurgical Examination of Blades

As-received and tested blades were examined to determine the condition of the edges and to determine whether any metallurgical changes occurred during engine operation. Since chromium, as well as the hardening elements titanium and aluminum, oxidizes more rapidly than the nickel in the Nimonic alloys, an impoverished layer, or depletion zone, is left on the surfaces exposed to hot combustion gases during high-temperature applications. Furthermore, since electropolishing could have an effect on the oxidation and subsequent depletion zone, studies were made of the edges of the blades after engine operation. Measurements were made of the thickness of oxidation, depth of oxide penetration, and depth of depletion in blades of each group. Standard metallurgical equipment and procedures were employed.

The mechanism of failure propagation was determined on the basis of the following definitions:

(1) Stress rupture: Stress-rupture blade failures are those occurring by cracking within the airfoil, by necking of the airfoil, or by fracturing in an irregular and jagged intercrystalline path. In addition to the main fracture, other similarly formed cracks frequently occurred near the origin of the main fracture or crack.

(2) Fatigue: Fatigue failures were those due to cracks that progressed from nucleation points, usually at or near either the leading or

trailing edges, in straight paths. The cracks were frequently smooth, often showed progression lines or concentric rings, and appeared to be transcrystalline.

(3) Stress rupture followed by fatigue: Blade failures that appeared to be caused by a combination of the preceding mechanisms were called stress rupture followed by fatigue. The fractured surfaces of blades in this group consisted of a small area that had the characteristics described for the stress-rupture category and a larger area with the fatigue characteristics. A further criterion was that other cracks also appeared immediately near the nucleation area of the main crack or fracture edge and appeared to be stress-rupture cracks.

In all cases, the blades failed finally in tension because of the progressive reduction in the load-carrying area, so that all blade failures showed a large area of rough fracture surface.

(4) Damage: Damaged blades were those showing nicks or dents in the airfoil that could have initiated the observed fracture. These blades were considered apart from the preceding three categories of blade failure, since they did not give a true indication of material properties.

RESULTS AND DISCUSSION

Engine Operating Results

The results of the cyclic engine test are presented in table III and figure 4. On the basis of the total range of blade life and the mean blade life of each group shown in figure 4, no appreciable improvement resulted from electropolishing precision-forged blades or machining oversize forged blades. Furthermore, no appreciable difference in the engine performance of the various lots of blades resulted.

Blade elongation during engine operation ranged up to a maximum of 0.5 percent in the middle portion of the blades. A typical blade-elongation curve is presented in figure 5 along with a typical curve of Stellite 21 for comparison. The creep in the Nimonic blades is negligible.

The location of failure origin and the mechanism of blade failure are shown in figure 6. Exclusive of the damage failures, it was determined that:

(1) A total of 45 percent of the blades failed by fatigue, 17 percent failed by stress rupture followed by fatigue, and 38 percent failed by stress rupture.

(2) Of all the blade failures, 65 percent originated at the leading edge.

(3) Of the blade failures originating at the leading edge, 42 percent were by stress rupture, 37 percent by fatigue, and 16 percent by stress rupture followed by fatigue.

(4) Of the blade failures originating at the trailing edge, 60 percent were by fatigue, 20 percent by stress rupture followed by fatigue, and 20 percent by stress rupture.

Metallurgical Studies of Blades Prior to Engine Operation

Photomicrographs of the edges of the various groups of blades prior to engine operation are presented in figure 7. The blades that were precision forged show a slightly oxidized, irregular surface 0.0005 inch thick (figs. 7(a) to (c)). These irregularities appear to be the result of external oxidation rather than intergranular oxidation. Typical edges of commercially electropolished blades of each lot are shown in figures 7(d) to (f). These blades were not sufficiently electropolished to remove the oxides completely and to smooth out the irregular surface. However, when the same blades were further electropolished (figs. 7(g) to (i)), the oxide was completely removed and the surface was smooth. The blades that were machined from oversize forgings had a clean and smooth surface free of distortion (fig. 7(j)).

Metallurgical Studies of Blades After Engine Operation

Photographs of the fracture edges of typical blade failures are presented in figure 8. An example of a fatigue-type failure is shown in figure 8(a), where the fracture follows a transcrystalline path, whereas the intercrystalline path of the fracture shown in figure 8(b) is typical of a stress-rupture failure.

Measurements of oxide penetration and depletion zones made on the last blade to fail in each group are presented in table IV, and several examples of the edges studied are shown in figure 9. The maximum oxide penetration and/or depletion zone appeared to be greatest in the blades that were electropolished. However, the typical or average depths of oxide penetration and depletion zone are not appreciably different.

Blade-Failure Mechanisms

Centrifugal stress and temperature are not the only service conditions that are known to limit the performance of turbine blades.

Blade vibrations may contribute to early failures by fatigue. Rapid heating or cooling may set up thermal stresses within the blades, and the action of the hot combustion gases may cause surface and intergranular corrosion.

In almost all cases, the classifications made by visual examination were supported by later microscopic examinations. A basic difficulty in defining the failure mechanism from the appearance of the fracture surface is that the effect of superimposed fatigue damage is not always evident. Reference 8, for example, reports measurements of high-temperature life of specimens subjected to vibratory loads superimposed upon constant loads. In many cases the fracture surface of the specimens showed no evidence of fatigue damage, although the reduction in life caused by the vibratory loads made it clear that fatigue must have been an important factor in causing early failure.

From the known distribution of temperature and centrifugal stress in the blade and from the known material properties, the stress-rupture life of material under the same combinations of centrifugally induced stress and temperature that exist along the length of the blade airfoil can be calculated. The results of such a calculation are presented in figure 1, where the stress-rupture life of Nimonic 80 bar stock given the standard heat-treatment is shown plotted against the distance above the base for the corresponding combinations of stress and temperature. The minimum in this curve shows that the most severe conditions, assuming stress-rupture conditions alone affect blade life, would be located 2.3 inches above the platform of the blades, where the stress is 18,000 pounds per square inch and the temperature is 1500° F. Furthermore, because of the material differences that exist between bar stock and forged blades, the stress-rupture life of the forged blades under stress-rupture conditions should not be expected to equal the minimum value given by figure 1. Only the location of the critical (minimum stress-rupture life) zone is considered in the following discussion.

Exclusive of the damage failures, the majority (65 percent) of failures originated at the leading edge of the blade and the balance at the trailing edge. Altogether 16 percent of the blades failed above the critical zone, 38 percent failed below, and 46 percent failed within the critical zone. From the macroexaminations and microexaminations of the fracture edges, the blade failures were classified as follows: 46 percent by fatigue, 38 percent by stress rupture, and 16 percent by stress rupture followed by fatigue. However, since the majority of failures in the critical zone, as well as in the zones above and below this portion of the airfoil, had fatigue characteristics, it may be concluded that fatigue played a predominant role in the failure mechanism of the various groups of blades.

Engine Operation

Since there was no appreciable difference in the operating life of the electropolished blades as compared with the precision-forged blades, it was concluded that electropolishing was not beneficial. The intergranular penetration of about 0.001 inch and oxide layer of about 0.0005 inch thickness on the surface of the precision-forged blades had no apparent harmful effect on the operating life of the blades. It is stated in reference 2 that intergranular oxide penetrations are harmful and that the damaged surface should be removed. However, the penetrations described in this reference were approximately 0.003 inch deep and resulted from solution-treating for 8 hours at 1080° C (1976° F) in an air atmosphere. The blades of the investigation reported herein were solution-treated for 8 hours at 1950° F in a natural gas atmosphere, and this may be the reason that the penetrations were relatively shallow.

Although the electropolished blades were clean and smooth prior to engine operation, the intergranular oxidation during engine operation appeared to penetrate electropolished blades to a greater maximum depth than precision-forged blades, as shown in figure 9 and table IV.

No improvement is made in the life of Refractaloy 26 alloy blades by coating, in spite of the fact that this alloy appeared susceptible to severe intergranular oxidation (ref. 3). In a previous investigation (ref. 4), electropolished blades had an engine operating life equivalent to forged blades for such alloys as Refractaloy 26, M-252, and Waspaloy.

In a fatigue test of precision-forged blades and blades machined from forged slugs (ref. 5), a substantial increase was noted in the fatigue properties of Nimonic 80 turbine blades as a result of machining blades from forged slugs. Although, as previously noted, fatigue played a predominant role in the blade failures in this engine, it was found that machining of oversize forged blades had no appreciable effect on the engine life of the blades when compared with precision-forged blades or electropolished blades. If the one blade of this group that failed early is omitted and a new mean life calculated on the basis of the remaining five blades, the sample would appear to be better than the precision-forged blades, and the improvement in mean life would be of the order of 25 percent. On the basis of these observations of the effect of electropolishing and of machining from oversize forgings, it may be concluded that the oxide penetration is not severe enough to be harmful to the blades or the blades are not as readily damaged by oxidation as was previously thought.

The notches that result from intergranular penetration of the oxides would not be expected to shorten the life of the blades in the zone of maximum failures where the temperature is 1500° F and the stress is

approximately 18,000 pounds per square inch since the Nimonic 80 alloys are not sensitive to notches under these conditions (ref. 9). However, on the basis of the temperature distribution along the blade (fig. 1), there is a notch-sensitive region 1 to $1\frac{1}{2}$ inches above the base. In this area of the blade, the temperature ranges from 1370° to 1450° F and the stress is approximately 20,000 pounds per square inch. In reference 9, it was shown that Nimonic 80A is notch-strengthened in rupture tests at 1200° F for times to rupture up to 1000 hours, and that at 1500° F no notch weakening should be observed at any time to rupture over 5 hours. In contrast, at 1300° and 1400° F pronounced notch weakening is observed at rupture times over 100 hours.

The first failure occurred in the Nimonic 80 (lot 2) precision-forged group after 81 hours of engine operation and originated $1\frac{1}{16}$ inches above the platform of the blade. All the blades in this group failed in the zone below 2 inches from the platform. The edges of this group of blades were the most irregular of any of the groups (fig. 7(b)). Of the seven groups of blades tested, the mean life of this group was the lowest. From these observations, it is possible that the irregularities and roughness of these blades greatly influenced the location of the origin of fracture within this group.

Although electropolishing had no appreciable effect on the mean life of this group of blades, conceivably, it could be beneficial under certain conditions. If the blade temperature of an engine in flight were about 1400° F, the blades could be in a notch-sensitive range for a period of time. In this instance, electropolishing or machining could minimize the notch effect and increase blade life.

CONCLUSIONS

An investigation of the engine performance of Nimonic 80 and Nimonic 80A turbine blades was conducted to determine the effect of electropolishing precision-forged blades and machining of blades from oversize forgings. These blades, along with precision-forged blades, were run in a J33-9 turbojet engine. On the basis of the results, it was concluded that:

1. Electropolishing of precision-forged blades did not improve engine life relative to the life of nonelectropolished blades.
2. Machining blades from oversize forgings did not improve the engine life of precision-forged blades.

3. The precision-forging and heat-treating practice used in fabricating the blades investigated was such that the surface roughness and oxide penetration were so slight, approximately 0.0005 inch in depth, as to preclude any benefits derived from surface removal by electro-polishing or machining.

4. The engine life of two lots of Nimonic 80 and one lot of Nimonic 80A blades did not vary appreciably and ranged from 81 hours to 200 hours. In general, fatigue played a predominant role in the failure mechanism of all groups of blades.

Lewis Flight Propulsion Laboratory
National Advisory Committee for Aeronautics
Cleveland, Ohio, January 21, 1955

REFERENCES

1. Hignett, H. W. G.: High Temperature Alloys in British Jet Engines. Paper presented at A.S.M. meeting (Detroit), Nov. 12, 1951. (Reprinted by The International Nickel Co., Inc.)
2. Pfeil, L. B., Allen, N. P., and Conway, C. G.: Nickel-Chromium-Titanium Alloys of the Nimonic 80 Type. Symposium on High-Temperature Steels and Alloys for Gas Turbines, Iron and Steel Inst. (London), July 1952, pp. 37-45.
3. Garrett, Floyd B., and Gyorgak, Charles A.: Adhesive and Protection Characteristics of Ceramic Coating A-417 and Its Effect on Engine Life of Forged Refractaloy-26 (AMS 5760) and Cast Stellite 21 (AMS 5385) Turbine Blades. NACA RM E52L30, 1953.
4. Clauss, F. J., Signorelli, R. A., and Johnston, J. R.: An Evaluation of Electropolished and Nonelectropolished Blades of Alloys Refractaloy 26, M-252, and Waspaloy in a J33-9 Turbojet Engine. NACA RM E54L29a.
5. Frith, P. H.: Fatigue Tests at Elevated Temperatures. Symposium on High-Temperature Steels and Alloys for Gas Turbines, Iron and Steel Inst. (London), July 1952, pp. 175-180.
6. Kemp, Richard H. and Morgan, William C.: Analytical Investigation of Distribution of Centrifugal Stresses and Their Relation to Limiting Operating Temperatures in Gas-Turbine Blades. NACA RM E7L05, 1948.

7. Morse, C. R., and Johnston, J. R.: Temperatures in a J47-25 Turbojet-Engine Combustor and Turbine Sections During Steady State and Transient Operation in a Sea-Level Test Stand. NACA RM E54K30a.
8. Ferguson, Robert R.: Effect of Magnitude of Vibratory Load Superimposed on Mean Tensile Load on Mechanism of and Time to Fracture of Specimens and Correlation to Engine Blade. NACA RM E52I17, 1952.
9. Brown, W. F., Jr., Jones, M. H., and Newman, D. P.: Influence of Sharp Notches on the Stress Rupture Characteristics of Several Heat Resistant Alloys: Pt. II. Preprint No. 67, A.S.T.M., 1953.

TABLE I. - CHEMICAL COMPOSITION OF ALLOYS

Element	Percent in -		
	Nimonic 80 (lot 1)	Nimonic 80 (lot 2)	Nimonic 80A
Carbon	0.05	0.024	0.05
Cobalt	0.44	0.37	0.30
Chromium	20.84	19.16	19.09
Nickel	74.92	75.05	75.41
Iron	0.55	0.50	0.31
Titanium	1.90	2.35	2.23
Aluminum	1.10	1.05	0.95
Silicon	0.04	0.35	0.13

TABLE II. - FORGING PROCEDURE AND HEAT TREATMENT

Precision forging (a)	Oversize forging
1. Heat to 2100° F in air	1. Heat to 2100° F in air
2. Upset and fuller	2. Upset and fuller
3. Reheat to 1920° F in natural gas atmosphere	3. Reheat to 1920° F in natural gas atmosphere
4. Press forge	4. Hammer forge
5. Water quench, wheel abrate, anodic etch	5. Water quench
6. Reheat to 1950° F in natural gas atmosphere	6. Reheat to 1920° F in natural gas atmosphere
7. Hammer forge (2000 lb)	7. Hammer forge (2000 lb)
8. Water quench, sand blast, anodic etch	8. Trim
9. Reheat to 1950° F in natural gas atmosphere	9. Water quench
10. Hot drop	10. Heat treatment: Nimonic 80 (lot 2) solution treated at 1985° F in natural gas atmosphere 8 hr; oil-quench aged at 1350° F in natural gas atmosphere 16 hr; air cooled
11. Air cool	11. Sand blast, inspect, sand blast
12. Heat treatment: Nimonic 80 (lot 1) + Nimonic 80A solution treated at 1950° F in natural gas atmosphere 8 hr; oil-quench aged at 1300° F in natural gas atmosphere 16 hr; air cooled. Nimonic 80 (lot 2) solution treated at 1985° F in natural gas atmosphere 8 hr; oil-quench aged at 1350° F in natural gas atmosphere 16 hr; air cooled	
13. Sand blast, inspect, sand blast, Tampico brush	

^aOne-half of each alloy group was electropolished in step 13.

TABLE III. - RESULTS OF ENGINE OPERATION OF TURBINE BLADES

Group	Failure time, hr at rated speed	Failure mechanism	Location of failure origin (a)	Distance of failure from root platform, in.
1 - Nimonic 80 (lot 1), precision forged	136.6	Fatigue	L.E.	$\frac{2}{8}$
	141.0	Damage	L.E.	$\frac{7}{16}$
	141.6	Damage	L.E.	$\frac{2}{8}$
	143.3	Fatigue	L.E.	$\frac{11}{16}$
	156.6	Stress rupture	L.E.	$\frac{1}{4}$
	174.8	Fatigue	T.E.	$\frac{2}{8}$
2 - Nimonic 80 (lot 1), electropolished	121.5	Damage	L.E.	$\frac{2}{4}$
	128.3	Fatigue	L.E.	$\frac{9}{16}$
	141.0	Stress rupture, fatigue	L.E.	$\frac{1}{2}$
	147.7	Fatigue	L.E.	$\frac{3}{4}$
	169.8	Damage	L.E.	$\frac{5}{8}$
	190.3	Damage	L.E.	$\frac{5}{8}$
3 - Nimonic 80A, precision forged	108.4	Damage	L.E.	$\frac{2}{4}$
	114.4	Stress rupture	L.E.	$\frac{3}{16}$
	116.5	Stress rupture	L.E.	$\frac{5}{16}$
	144.3	Stress rupture	L.E.	$\frac{3}{8}$
	145.2	Damage	L.E.	$\frac{1}{4}$
	156.6	Damage	L.E.	$\frac{3}{8}$
4 - Nimonic 80A, electropolished	126.7	Fatigue	L.E.	$\frac{5}{8}$
	142.9	Stress rupture, fatigue	L.E.	$\frac{3}{8}$
	144.3	Fatigue	L.E.	$\frac{3}{4}$
	148.3	Fatigue	T.E.	$\frac{2}{2}$
	154.8	Stress rupture, fatigue	L.E.	$\frac{5}{8}$
	160.5	Stress rupture	L.E.	$\frac{1}{8}$
5 - Nimonic 80 (lot 2), precision forged	80.8	Fatigue	T.E.	$\frac{1}{16}$
	91.6	Stress rupture, fatigue	T.E.	$\frac{1}{4}$
	108.3	Stress rupture	T.E.	$\frac{1}{2}$
	141.6	Fatigue	T.E.	$\frac{1}{8}$
	147.7	Fatigue	T.E.	$\frac{5}{8}$
	170.4	Stress rupture	L.E.	$\frac{7}{8}$
6 - Nimonic 80 (lot 2), electropolished	92.7	Damage	L.E.	$\frac{2}{8}$
	108.3	Damage	---	--
	116.5	Stress rupture	L.E.	$\frac{7}{8}$
	141.0	Stress rupture	L.E.	$\frac{7}{16}$
	152.5	Damage	L.E.	$\frac{1}{8}$
	180	Stress rupture	L.E.	$\frac{1}{8}$
7 - Nimonic 80 (lot 2), forged oversize and machined	91.6	Fatigue	T.E.	$\frac{1}{8}$
	170.4	Damage	L.E.	$\frac{1}{2}$
	172.8	Fatigue	T.E.	$\frac{3}{16}$
	191.5	Damage	L.E.	$\frac{3}{8}$
	194.3	Stress rupture, fatigue	T.E.	$\frac{1}{16}$
	199.6	Stress rupture	L.E.	$\frac{3}{16}$

L.E. - leading edge.
T.E. - Trailing edge.

TABLE IV. - MEASUREMENTS OF SURFACE EFFECTS AFTER ENGINE OPERATION

[All measurements made on specimens cut about 1/4 in. below fracture edge of last blade failure in each group.]

Group	Alloy	Condition	Failure time, hr at rated speed	Oxide penetration, in.		Depletion zone, in.	
				Typical	Maximum	Typical	Maximum
1	Nimonic 80 (lot 1)	Precision forged	174.8	0.0015	0.0018	0.0026	0.0030
2	Nimonic 80 (lot 1)	Electropolished	147.7	.0021	.0026	.0032	.0035
3	Nimonic 80A	Precision forged	144.3	.0014	.0016	.0029	.0030
4	Nimonic 80A	Electropolished	180.5	.0010	.0029	.0016	.0032
5	Nimonic 80 (lot 2)	Precision forged	170.4	.0011	.0013	.0016	.0018
6	Nimonic 80 (lot 2)	Electropolished	180.0	.0011	.0058	.0014	.0018
7	Nimonic 80 (lot 2)	Forged oversize, machined	199.6	.0014	.0017	.0018	.0019

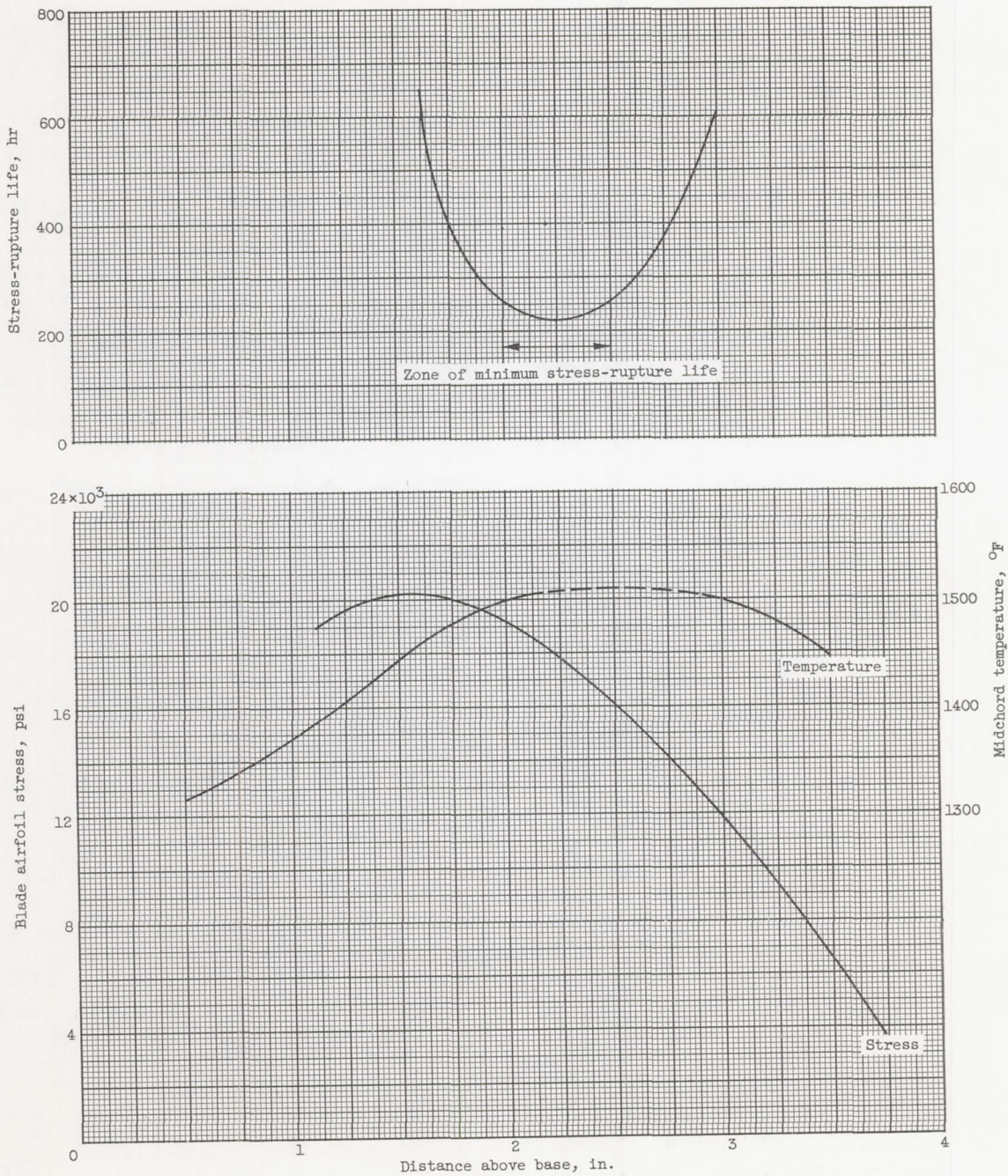


Figure 1. - Typical stress and temperature distribution of airfoil of J33-9 turbine blade of Nimonic 80 alloy.

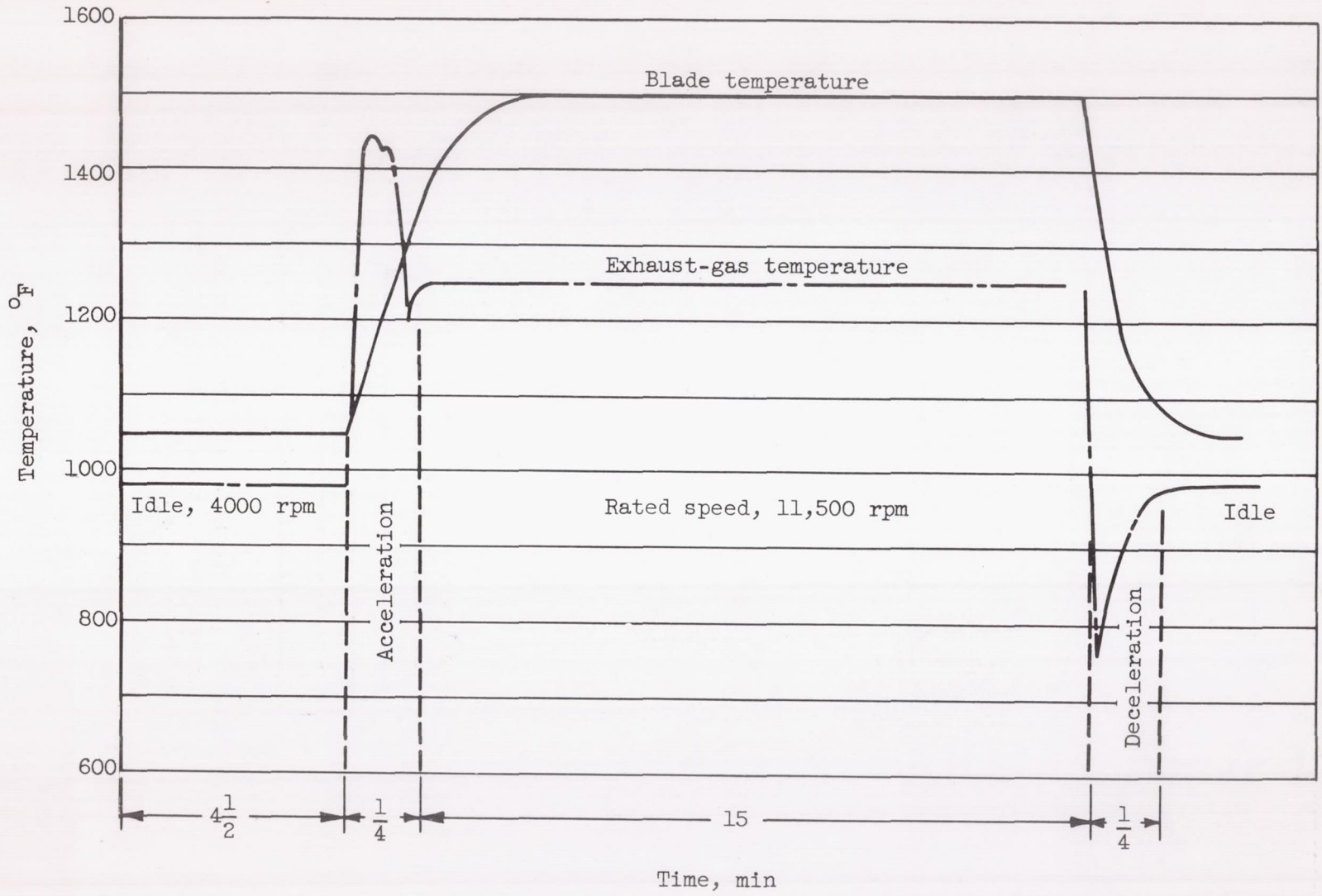


Figure 2. - Temperature conditions during typical engine cycle. (Dimensions are in inches.)

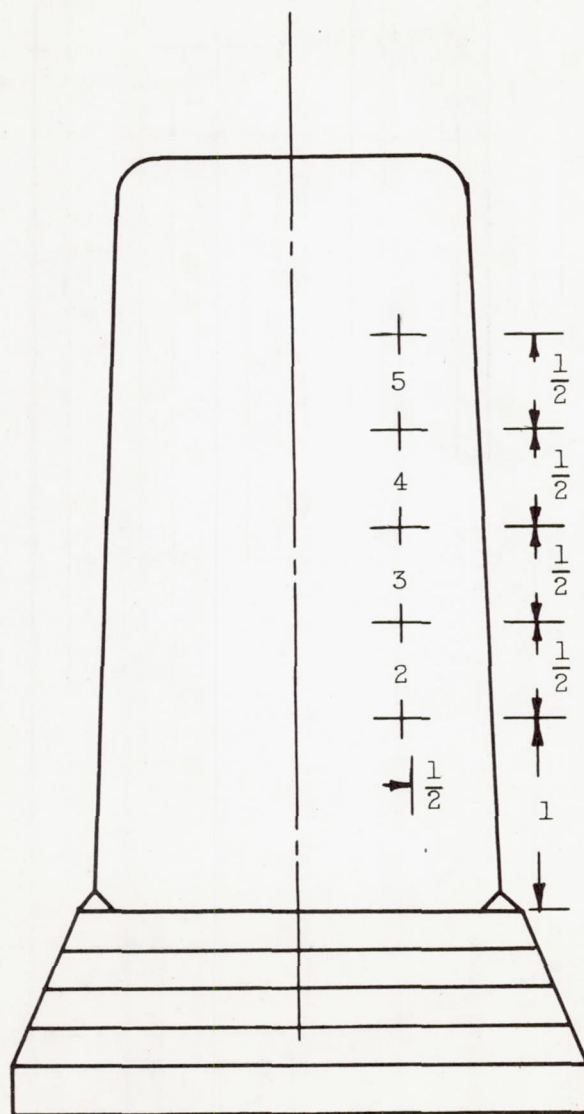


Figure 3. - Location of scribe marks on convex side of turbine blades for use in measuring elongation. (Dimensions are in inches.)

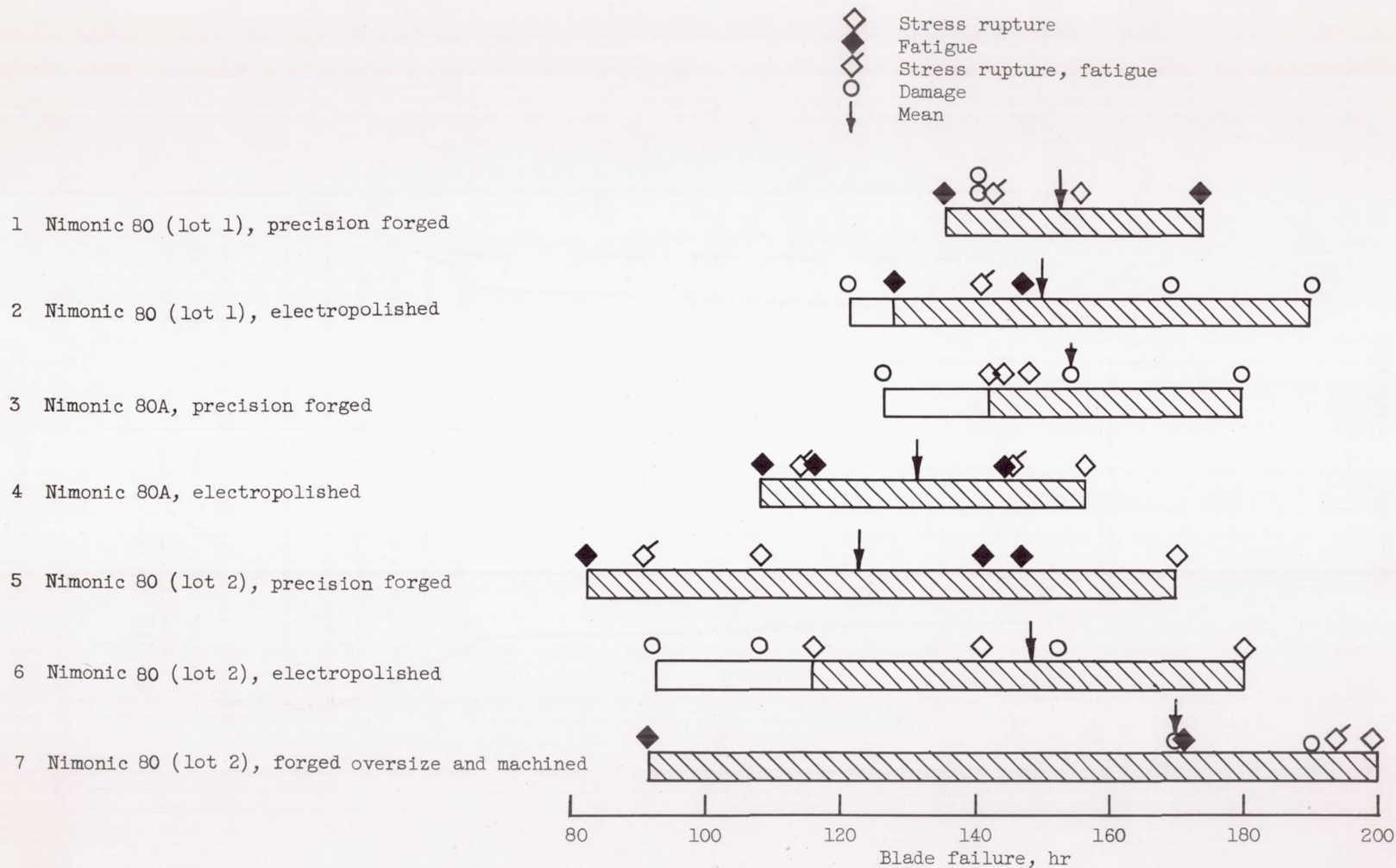


Figure 4. - Results of engine operation.

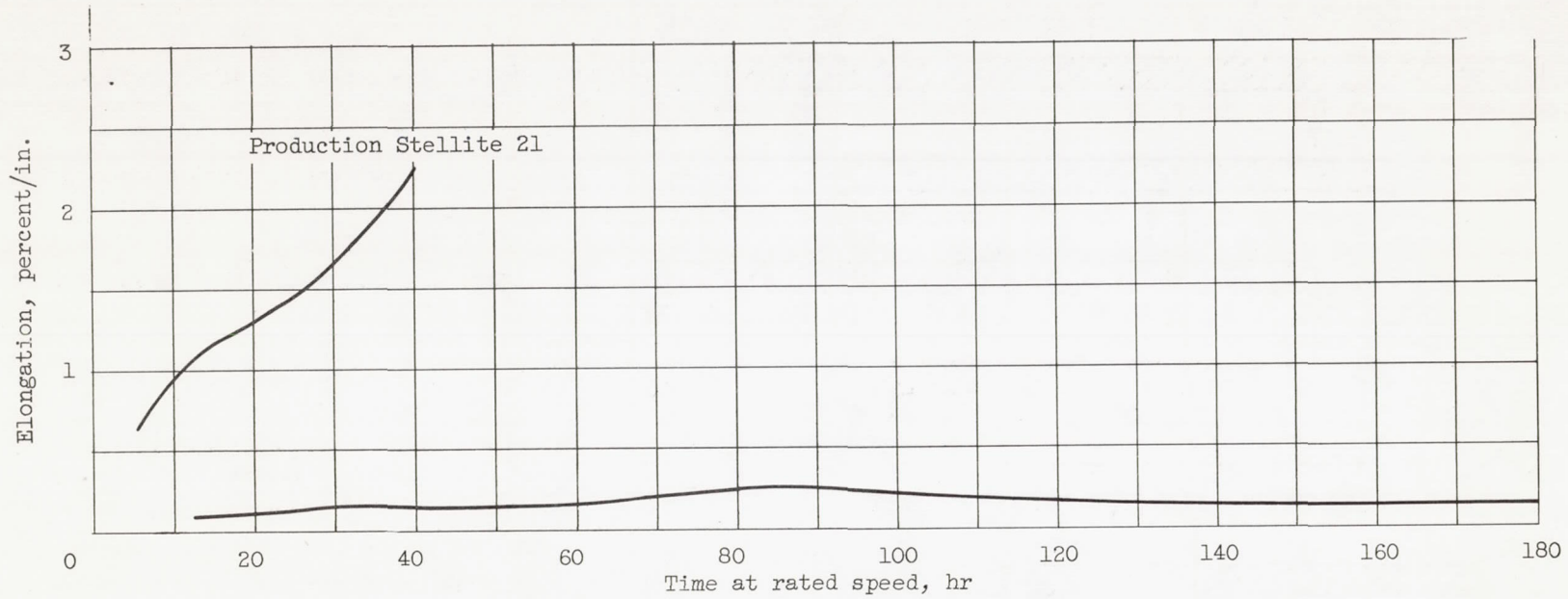


Figure 5. - Typical elongation in zones 3 and 4 of Nimonic 80 alloy blades.

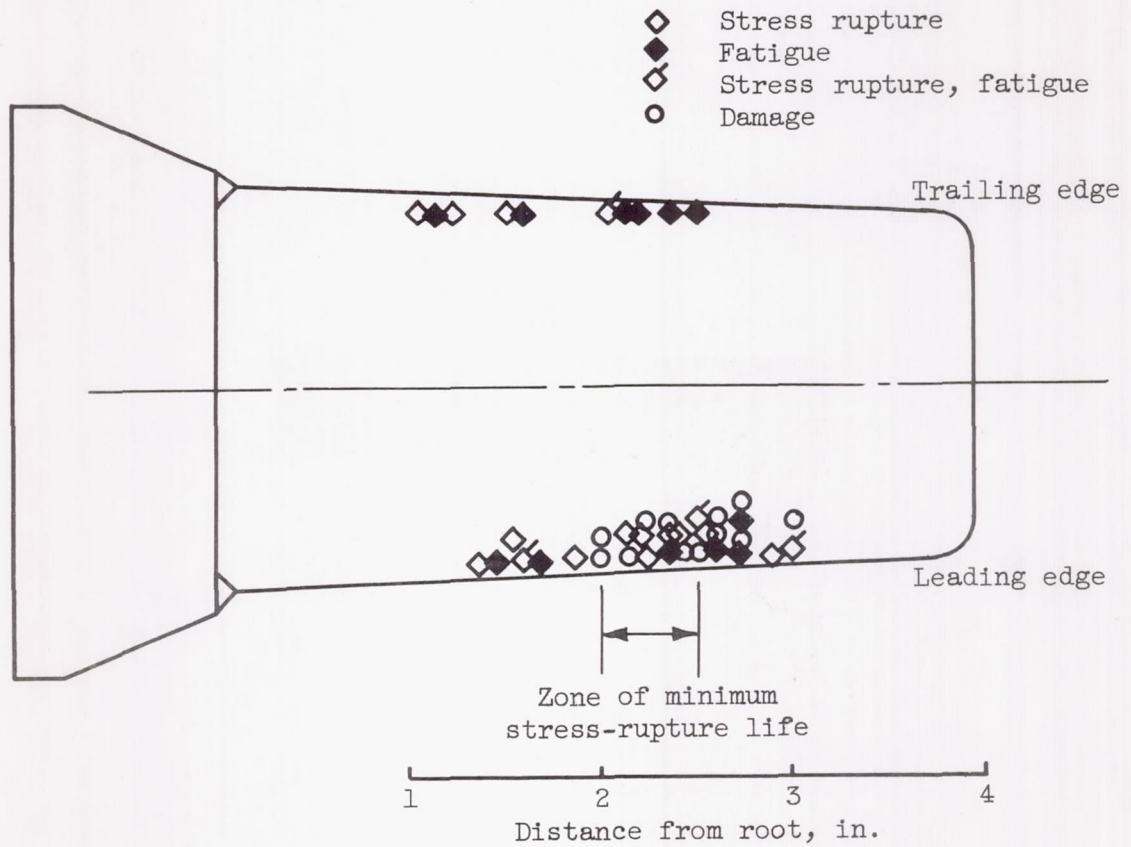
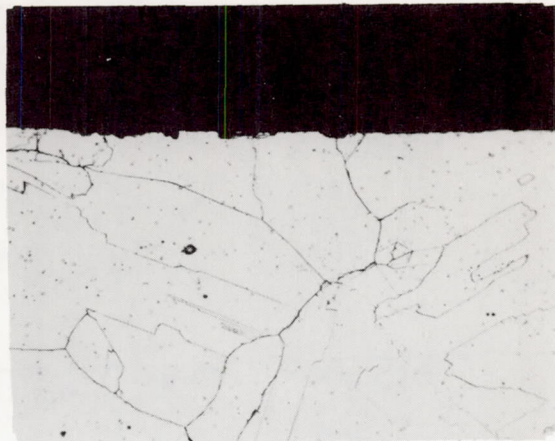
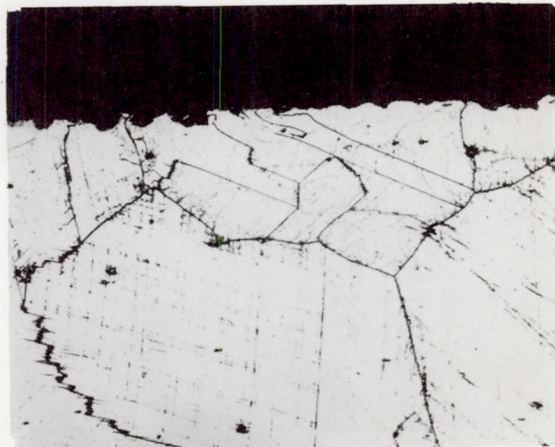


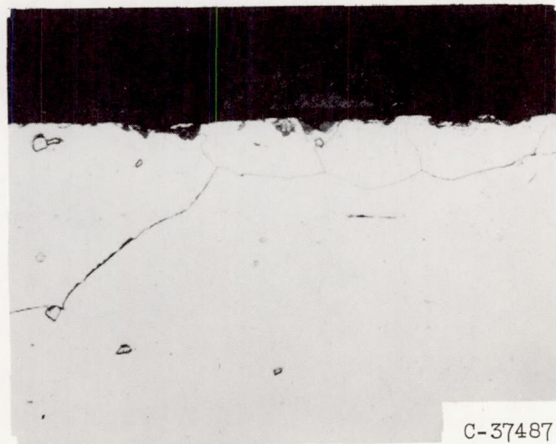
Figure 6. - Location of blade-failure origins and mechanism of blade failures.



(a) Nimonic 80 (lot 1); precision forged.

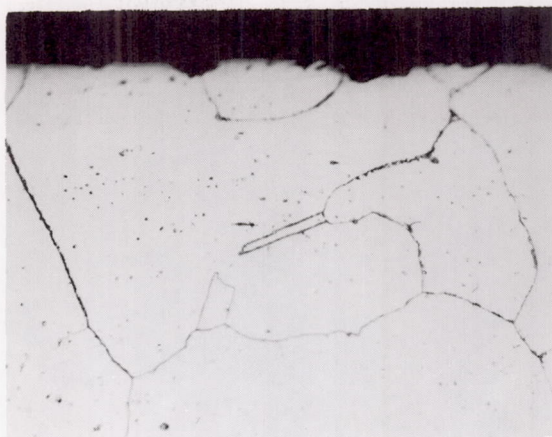


(b) Nimonic 80 (lot 2); precision forged.

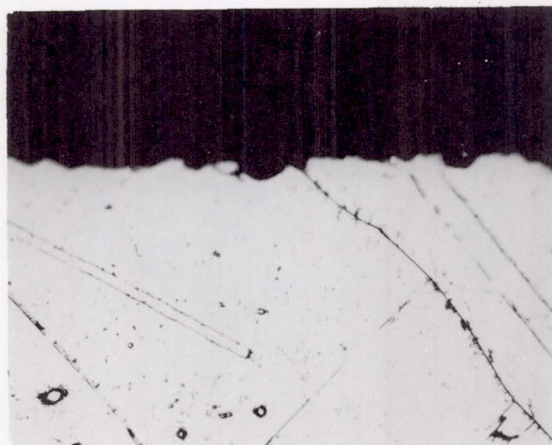


(c) Nimonic 80A; precision forged.

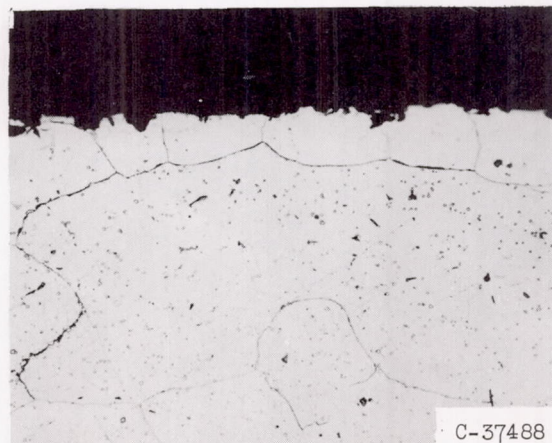
Figure 7. - Typical blade edges prior to engine operation. X500.



(d) Nimonic 80 (lot 1); commercial electropolish.

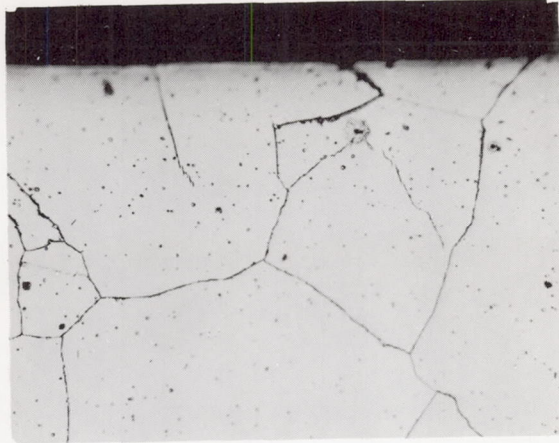


(e) Nimonic 80 (lot 2); commercial electropolish.

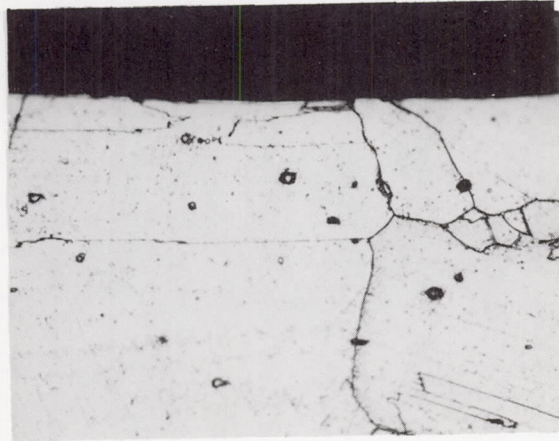


(f) Nimonic 80A; commercial electropolish.

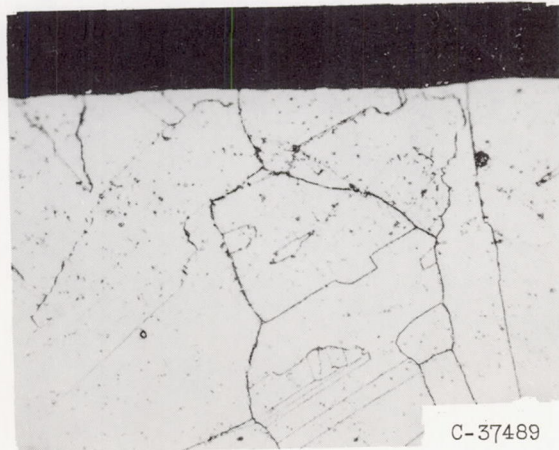
Figure 7. - Continued. Typical blade edges prior to engine operation. X500.



(g) Nimonic 80 (lot 1); NACA electropolish.

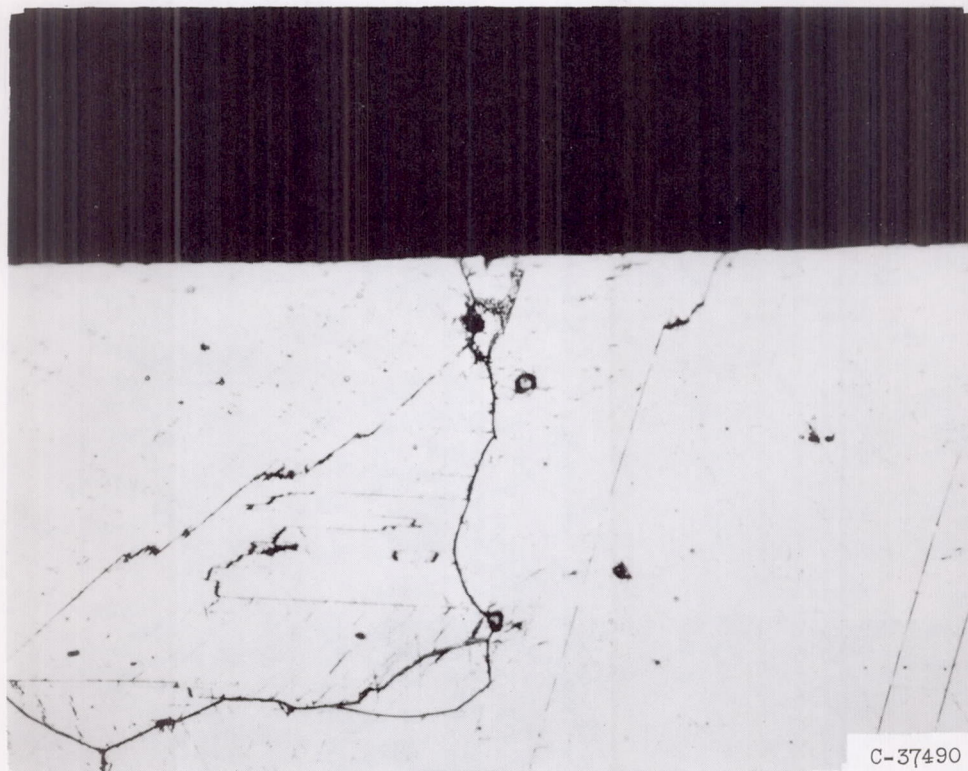


(h) Nimonic 80 (lot 2); NACA electropolish.



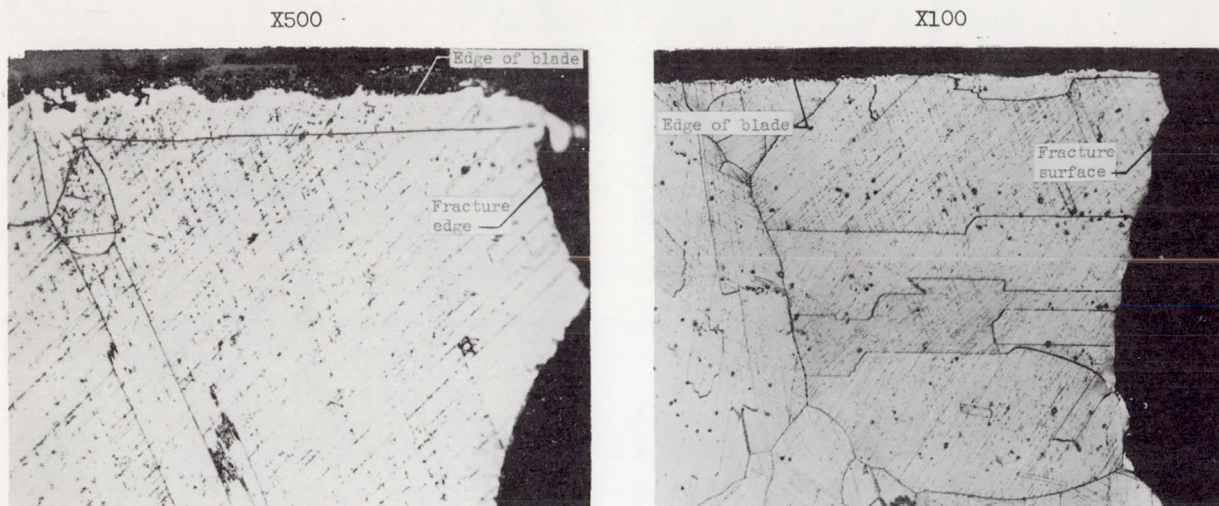
(i) Nimonic 80A; NACA electropolish.

Figure 7. - Continued. Typical blade edges prior to engine operation. X500.

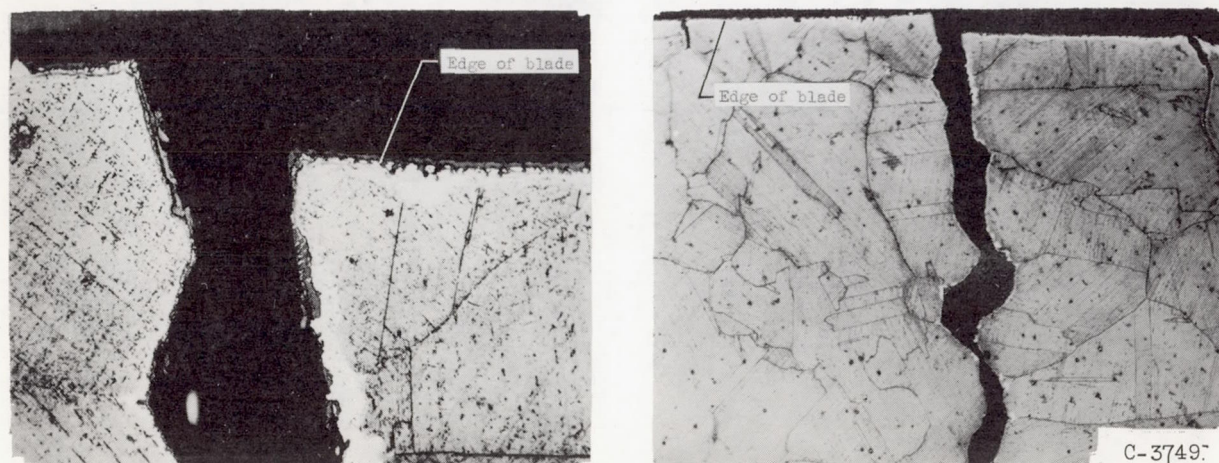


(j) Nimonic 80 (lot 2); etchant: 20 parts hydrofluoric acid, 20 parts glycerin, and 5 parts water; forged oversize and machined.

Figure 7. - Concluded. Typical blade edges prior to engine operation. X500.

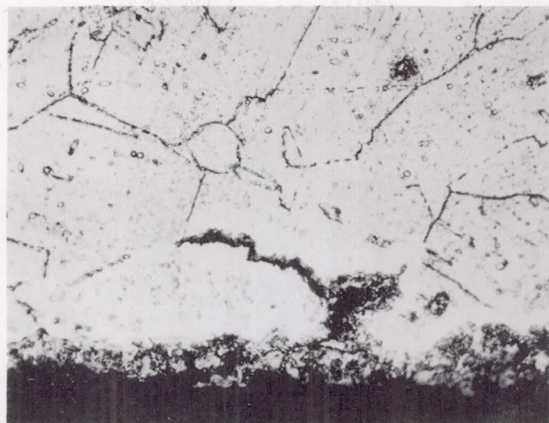


(a) Fatigue-type failure.

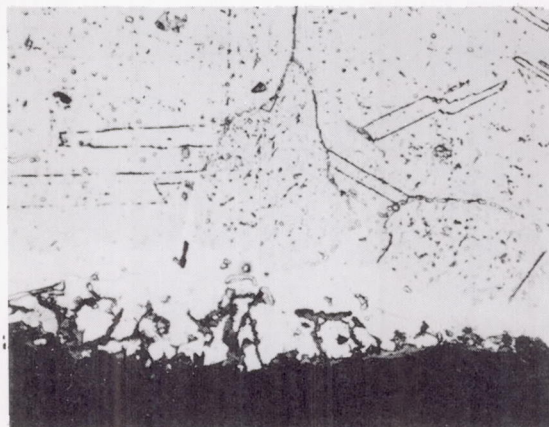


(b) Stress-rupture-type failure.

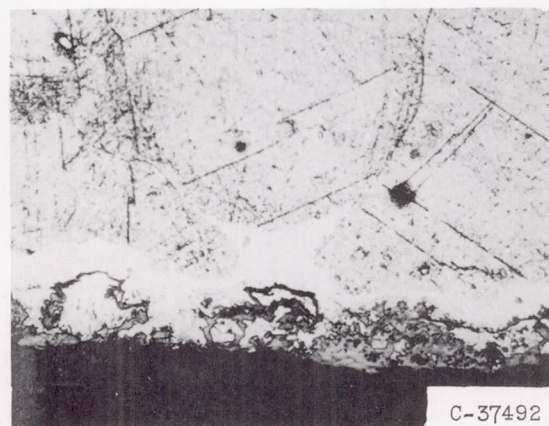
Figure 8. - Typical blade failures. Etchant: 20 parts hydrofluoric acid, 20 parts glycerin, and 5 parts water.



(a) Maximum oxide penetration.



(b) Typical depletion zone and oxide penetration.



(c) Maximum depletion zone.

Figure 9. - Typical edges of blades after engine operation.
Etchant, 20 parts hydrofluoric acid, 20 parts glycerin,
and 5 parts water. X750.

Name: _____
 ID: _____
 Signature: _____
 Date: _____

Name: _____
 ID: _____
 Signature: _____
 Date: _____

Time	Temperature	Pressure	Flow Rate	Concentration	Retention Time	Peak Identification
0.0	25.0	1.0	1.0	0.0	0.0	None
1.0	25.0	1.0	1.0	0.0	0.0	None
2.0	25.0	1.0	1.0	0.0	0.0	None
3.0	25.0	1.0	1.0	0.0	0.0	None
4.0	25.0	1.0	1.0	0.0	0.0	None
5.0	25.0	1.0	1.0	0.0	0.0	None
6.0	25.0	1.0	1.0	0.0	0.0	None
7.0	25.0	1.0	1.0	0.0	0.0	None
8.0	25.0	1.0	1.0	0.0	0.0	None
9.0	25.0	1.0	1.0	0.0	0.0	None
10.0	25.0	1.0	1.0	0.0	0.0	None
11.0	25.0	1.0	1.0	0.0	0.0	None
12.0	25.0	1.0	1.0	0.0	0.0	None
13.0	25.0	1.0	1.0	0.0	0.0	None
14.0	25.0	1.0	1.0	0.0	0.0	None
15.0	25.0	1.0	1.0	0.0	0.0	None
16.0	25.0	1.0	1.0	0.0	0.0	None
17.0	25.0	1.0	1.0	0.0	0.0	None
18.0	25.0	1.0	1.0	0.0	0.0	None
19.0	25.0	1.0	1.0	0.0	0.0	None
20.0	25.0	1.0	1.0	0.0	0.0	None
21.0	25.0	1.0	1.0	0.0	0.0	None
22.0	25.0	1.0	1.0	0.0	0.0	None
23.0	25.0	1.0	1.0	0.0	0.0	None
24.0	25.0	1.0	1.0	0.0	0.0	None
25.0	25.0	1.0	1.0	0.0	0.0	None